

This article was downloaded by: [Georgia State University]

On: 14 September 2009

Access details: Access Details: [subscription number 906453965]

Publisher Taylor & Francis

Informa Ltd Registered in England and Wales Registered Number: 1072954 Registered office: Mortimer House, 37-41 Mortimer Street, London W1T 3JH, UK



## Research in Sports Medicine

Publication details, including instructions for authors and subscription information:

<http://www.informaworld.com/smpp/title-content=t713926139>

### An Instrumented Wheel System for Measuring 3-D Pushrim Kinetics During Racing Wheelchair Propulsion

Weerawat Limroongreungrat <sup>a</sup>; Yong Tai Wang <sup>a</sup>; Li-shan Chang <sup>a</sup>; Mark D. Geil <sup>b</sup>; Jeffery T. Johnson <sup>c</sup>

<sup>a</sup> Division of Physical Therapy, Georgia State University, Atlanta, Georgia, USA <sup>b</sup> Department of Kinesiology and Health, Georgia State University, Atlanta, Georgia, USA <sup>c</sup> Department of Physical Education and Recreation, University of West Georgia, Carrollton, Georgia, USA

Online Publication Date: 01 July 2009

**To cite this Article** Limroongreungrat, Weerawat, Wang, Yong Tai, Chang, Li-shan, Geil, Mark D. and Johnson, Jeffery T. (2009) 'An Instrumented Wheel System for Measuring 3-D Pushrim Kinetics During Racing Wheelchair Propulsion', *Research in Sports Medicine*, 17:3, 182 — 194

**To link to this Article:** DOI: 10.1080/15438620903120637

**URL:** <http://dx.doi.org/10.1080/15438620903120637>

PLEASE SCROLL DOWN FOR ARTICLE

Full terms and conditions of use: <http://www.informaworld.com/terms-and-conditions-of-access.pdf>

This article may be used for research, teaching and private study purposes. Any substantial or systematic reproduction, re-distribution, re-selling, loan or sub-licensing, systematic supply or distribution in any form to anyone is expressly forbidden.

The publisher does not give any warranty express or implied or make any representation that the contents will be complete or accurate or up to date. The accuracy of any instructions, formulae and drug doses should be independently verified with primary sources. The publisher shall not be liable for any loss, actions, claims, proceedings, demand or costs or damages whatsoever or howsoever caused arising directly or indirectly in connection with or arising out of the use of this material.

# An Instrumented Wheel System for Measuring 3-D Pushrim Kinetics During Racing Wheelchair Propulsion

WEERAWAT LIMROONGREUNGRAT, YONG TAI WANG,  
and LI-SHAN CHANG

*Division of Physical Therapy, Georgia State University, Atlanta, Georgia, USA*

MARK D. GEIL

*Department of Kinesiology and Health, Georgia State University, Atlanta, Georgia, USA*

JEFFERY T. JOHNSON

*Department of Physical Education and Recreation, University of West Georgia,  
Carrollton, Georgia, USA*

*The purpose of this study was to design and validate an instrumented wheel system (IWS) that can measure 3-dimensional (3-D) pushrim forces during racing wheelchair propulsion. Linearity, precision, and percent error were determined for both static and dynamic conditions. For the static condition, the IWS demonstrated a high linearity ( $0.91 \leq \text{slope} \leq 1.41$ ) with less than 2.72% error rate. Under dynamic loading, the IWS provided the well-matched measurement forces with the predicted values from the inverse dynamics method ( $0.96 \leq \text{slope} \leq 1.07$ ) with less than 4.32% error rate. The results revealed that the IWS developed in the study can be used to measure 3-D pushrim reaction forces with acceptable accuracy. This was the first instrumented wheel device that can register 3-D pushrim forces during racing wheelchair propulsion. With the available kinetic information of the 3-D pushrim forces, the upper extremity joint reaction forces could be determined.*

---

Received 30 April 2008; accepted 23 December 2008.

The authors thank Mr. Fran Edel for his help in constructing the instrumented wheel system, and Dr. Lauri Malone, Coach Kevin Orr, and athletes from Lakeshore Foundation, Birmingham, Alabama, for their help in experiments.

Address correspondence to Yong 'Tai' Wang, Ph.D., Division of Physical Therapy, Georgia State University, 140 Decatur Street, Urban Life Building, Room 1279, Atlanta, GA 30302-3995, USA. E-mail: ywang2@gsu.edu

*KEYWORDS* kinetics, instrumented wheel system, racing wheelchair propulsion, 3-D forces

## INTRODUCTION

Biomechanical studies can gain insight into the causes and consequences of high loads on the upper extremity during conventional wheelchair propulsion. Although in the last two decades researchers have examined kinematic and kinetic aspects involved in conventional wheelchairs and other sport/recreational wheelchairs, direct measurements of the pushrim reaction forces during racing wheelchairs propulsion is limited (Asato et al. 1993; Finley et al. 2004; Wu et al. 1998). This limitation mainly is due to the complexity of developing a reliable measurement system to measure three-dimensional (3-D) forces and moments at the pushrim, since racing wheelchairs have different structures and designs than daily conventional wheelchairs (Asato et al. 1993; Wu et al. 1998). The valid measurement of 3-D pushrim reaction forces, however, would provide the basis to predict the wrist, elbow, and shoulder joint reaction forces during racing wheelchair propulsion. These predictions can lead to a better understanding of the mechanisms of injury, allowing for the improvement or modification of racing wheelchair propulsion techniques and reduction of risk to the joints of the upper extremity.

Only a few research groups have developed instrumented wheel systems (IWSs) to measure 3-D forces and moments during conventional wheelchair propulsion for daily wheelchair use (Asato et al. 1993; Finley et al. 2004; Wu et al. 1998). SMART<sup>Wheel</sup>, developed by a research team led by Dr. Cooper from the University of Pittsburgh, is the first IWS that is capable of registering 3-D forces during conventional wheelchair propulsion. The SMART<sup>Wheel</sup> is now commercially available. The system consists of a 2.4 GHz Wi-Fi 802.11b wireless access point that can be plugged into a standard ethernet network interface card, allowing a data collection range up to 300 ft indoors and 500 ft outdoors. The percent linearity for the moment and force were found to be 99.1% and 98.9%, respectively (VanSickle, Cooper, and Robertson 1995).

Wu et al. (1998) develop an IWS to measure pushrim forces during conventional wheelchair propulsion using a commercial 6 DOF force-transducer (JR-3 Inc., Woodland, CA). The system incorporates a data logger and a handrim unit mounted on a wheel hub. Excellent validity of the IWS is reported for both static and dynamic conditions on daily conventional wheelchairs (Wu et al. 1998). To date, only one study reports the development of IWS to measure pushrim forces during racing wheelchair propulsion (Goosey-Tolfrey et al., 2001). Nevertheless, this system can measure only two-dimensional forces and tangential and medial-lateral components. Racing wheelchair propulsion involves 3-D movements, and the radial force provides useful information on frictional forces between the hand and

pushrim (Cooper 1995). Without the available kinetic information of the 3-D pushrim reaction forces during racing wheelchair propulsion, the upper extremity joint reaction forces could not be accurately computed or estimated. These joint reaction forces can provide crucial information related to mechanisms of injury, so that the racing wheelchair propulsion techniques can be modified or significantly improved.

Therefore, the purpose of the study is to develop a valid IWS using a commercial force transducer to measure the 3-D pushrim reaction forces on a racing wheelchair during racing wheelchair propulsion. These measurements provide the essential kinetic information for the future inverse dynamics method of racing wheelchair propulsion.

## METHODS

### Instrumented Wheel System

This IWS was composed of a 3-D JR3 force transducer (model 45E15A-U760, JR-3, Inc., Woodland, CA), the interface plate, the rear wheel, the pushrim, and the slip-ring unit. How the IWS was assembled is presented in Figure 1.

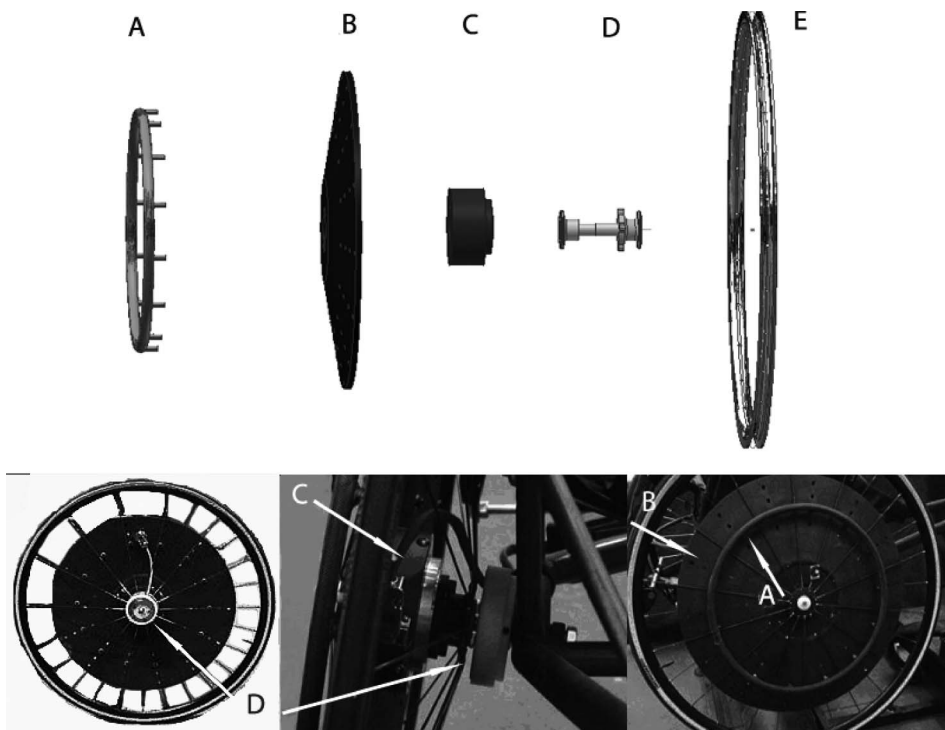


**FIGURE 1** A diagram represents the instrumented wheel system: (A) pushrim; (B) interface plate; (C) 3-D force transducer; (D) hub, slip-ring and its retainer; (E) wheel.

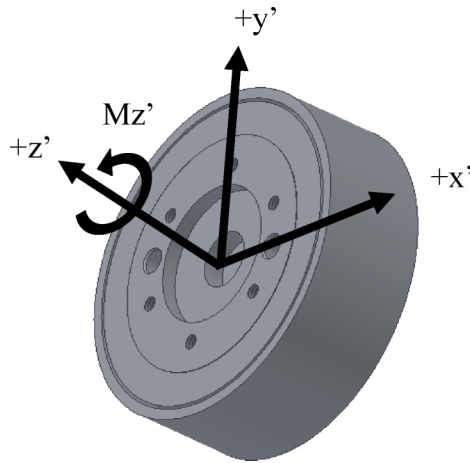


**FIGURE 2** Coordinate system for the force transducer ( $x'$ ,  $y'$ ,  $z'$ ). In-plane axes,  $x'$  and  $y'$ , are perpendicular to each other; outer plane axis,  $z'$ , is perpendicular to  $x'y'$  plane.  $Mz'$  is also perpendicular to  $x'y'$  plane, and is used to define propulsion phase.

This transducer had a full mechanical loading rate of 1113 N for in-plane ( $x'$  and  $y'$ , which are perpendicular to each other, Figure 2) axes, 2226 N for the outer plane ( $z'$ , perpendicular to  $x'y'$  plane) axis, and 127 N·m of moments for all directions. The transducer was mounted inside of the rear wheel hub in order to avoid any hindrance to propulsion mechanics. The interface plate, made of aluminum (T6061), was 46.9 cm in diameter and 0.635 cm in thickness, and had the slope of  $10^\circ$  from the center. The interface plate was mounted directly to the force transducer without connecting to other parts of the wheel. Four different sets of 14-holes, with the diameter of 6.35 mm, were drilled on the interface plate to match with different pushrim lug sizes (30.48, 35.56, 40.64, and 45.72 cm diameter). The slip-ring unit consisted of a slip-ring and a slip-ring retainer. The slip-ring used in this study was a 10-track disc slip-ring (The Sibley Company, Haddam, CT, USA) with a 4.62 cm bore and outer diameter of 7.36 cm. The slip-retainer was made of ultrahigh molecular weight polyethylene (UHMW-PE) since it is lightweight and nonconductive. Moreover, this material had a high impact strength, abrasion, and wear resistance.

The IWS was connected to the A/D interface unit of the Peak Performance system (Peak Performance Technologies, Inc., Englewood, CO, USA), which allowed the system to be synchronized with multiple optical cameras via a 5 V transistor-transistor logic (TTL), which served as a trigger device.

### Coordinate Systems and Force Determination

The forces in this system are defined in three coordinate systems, including the transducer coordinate system ( $x'$ ,  $y'$ ,  $z'$ ), the global coordinate system

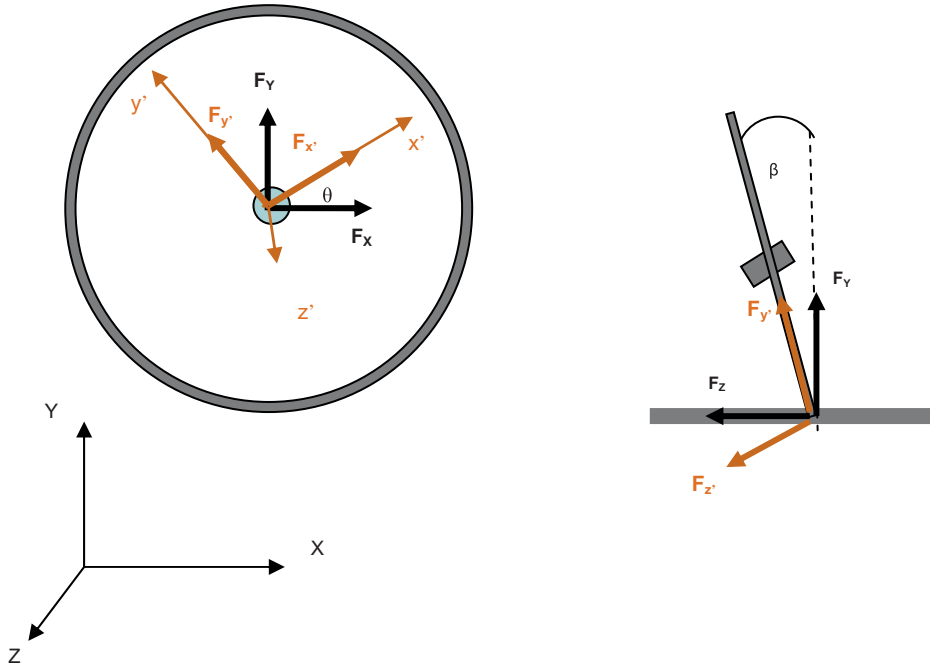


**FIGURE 3** Transducer ( $x', y', z'$ ) and global ( $X, Y, Z$ ) coordinate systems. The force components in the transducer coordinate system are converted to the global coordinate system, where  $\beta$  is the camber angle.

( $X, Y, Z$ ), and the pushrim coordinate system ( $r, t, z$ ). The force components in the transducer coordinate system can be converted to the global coordinate system by the following:

$$\begin{bmatrix} F_X \\ F_Y \\ F_Z \end{bmatrix} = \begin{bmatrix} \cos \theta \cos \beta & -\sin \theta \cos \beta & 0 \\ \sin \theta \cos \beta & \cos \theta \cos \beta & 0 \\ 0 & 0 & \cos \beta \end{bmatrix} \begin{bmatrix} F_{x'} \\ F_{y'} \\ F_{z'} \end{bmatrix}, \tag{1}$$

where  $\beta$  is a camber angle and  $\theta$  is the angle between the direction of  $x'$  and  $X$  (Figure 3).

The force components in the global coordinate system can be converted to the pushrim coordinate system by the following (Figure 4):

$$F_t = F_X \sin \theta \cos \beta - F_Y \sin \theta \cos \beta + F_Z \sin \theta \sin \beta, \tag{2}$$

$$F_z = F_z \sin \beta. \tag{3}$$

Since  $F_{total}^2 = F_X^2 + F_Y^2 + F_Z^2 = F_t^2 + F_r^2 + F_z^2$ , then  $F_r$  can be determined as

$$F_r = \sqrt{F_{total}^2 - F_t^2 - F_z^2}. \tag{4}$$

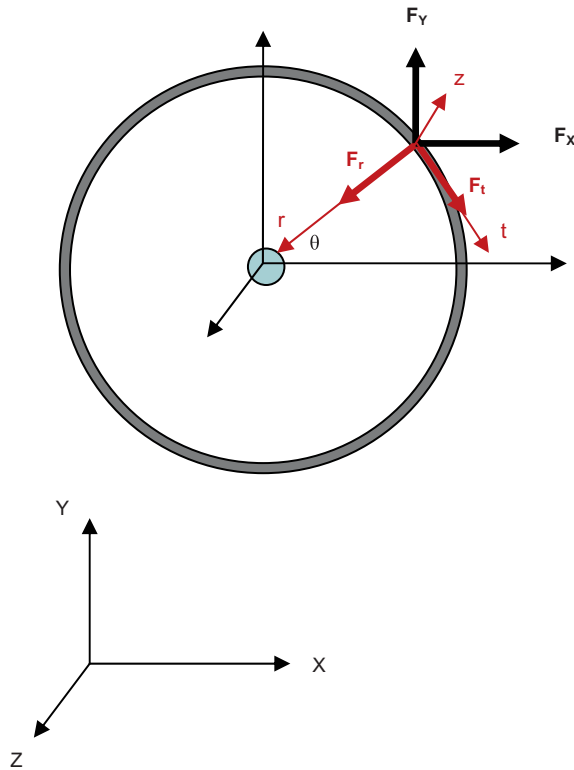


**FIGURE 4** Global (X, Y, Z) and pushrim (t, r, z) coordinate systems. The force components in the global coordinate system are converted to the pushrim coordinate system.

### System Validation

For static validation, the IWS was vertically mounted to the wheel stand so that the forces associated with the  $x'$  and  $y'$  of the force transducer could be measured. Five different reference loads (24.02, 46.26, 68.50, 90.74, and 112.98 N) were suspended from the pushrim at eight specified positions that were  $45^\circ$  apart along the circumference of the pushrim. Five trials were collected for 3 seconds in each position. The measured values from the IWS were compared with the reference loads.

Dynamic validation was processed by using an electrical motor to spin the instrumented wheel at two different constant speeds (since the motor has two speed modes, 1.46 and 7.15 rad/s), while the IWS was vertically mounted on the wheel stand. This testing position was the same as the static validation position. Two different metal blocks with the mass of 2.04 and 3.48 Kg were attached on the pushrim one at a time by a hose clamp, and were used to validate the IWS in different weight conditions. These measured forces ( $F_x$  and  $F_y$ ) were compared with

reference forces obtained from the inverse dynamics method. The forces from the inverse dynamics method can be obtained from centripetal force ( $F_c$ ) of uniform vertical circular motion from the following equation:

$$\sum F_c = N \pm w = mr\omega^2, \tag{5}$$

where  $N$  is a normal force,  $w = m_{metal\ block} \cdot g \cos\theta$ , and  $\theta$  is the angle between the direction of gravity and  $N$ . Once, the centripetal force ( $F_c$ ) was determined, the reference forces in X and Y can be calculated (Figure 5).

A 120-Hz Peak Performance optical camera, aligned perpendicular to the rotating plane, was used to capture kinematic data. Three retroreflective markers (8 mm) were placed on the IWS, one at the center of the wheel, one on the interface plate, and the last one on the metal block. The last two retroreflective markers were aligned in the same direction of

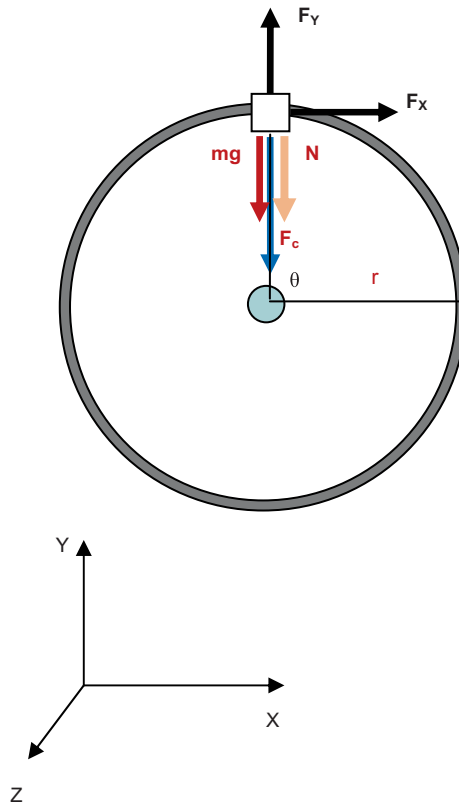


**FIGURE 5** Free-body diagram of centripetal force ( $F_c$ ) that derived from uniform vertical circular motion.

JR-3 force transducer +x' axis and were used to obtain angular wheel position. Kinematic and kinetic systems were connected to A/D interface unit of the Peak Performance system and were synchronized via the trigger device. An acquisition software program was used to obtain analog, coordinate data, and filter raw data. A second-order Butterworth digital filter was used to smooth the raw kinematic data with a 7-Hz cut-off frequency. The dynamic validation consisted of five trials for each condition (two different loads vs. two different velocities). Twenty trials in total were collected.

Linearity, coefficients of determination, precision, and percent error were determined for both static and dynamic conditions. Linearity was reported as the slope of linear regression analysis between measured forces and reference forces. Precision was obtained from standard deviation of each measurement. Finally, percent error was determined from relative percent error, which was the difference between measured force and reference force divided by the reference force and then multiplied by 100%.

### Human Participant Test

To demonstrate practicability, the IWS was mounted to the right side of standard racing wheelchair with a wheel camber angle of 10°. The wheelchair was secured on a wheelchair stationary roller. An experienced racing wheelchair athlete, who had a bilateral above the knee amputation, volunteered to propel the wheelchair at a speed comfortable to him (5.0–5.5m/s). Prior to data collection, the athlete read and signed a consent form that followed the guidelines of the Institutional Review Board. Three retroreflective markers were placed on the right hand, which corresponded to the second metacarpophalangeal joint (MCP2), the fifth metacarpophalangeal joint (MCP5), and the midpoint between radial and ulna styloid process (MW). Two other retroreflective markers (8 mm) were placed on the IWS: one at the center of the wheel and one on the interface plate, which aligned in the same direction of +x' axis of JR-3 force transducer in order to obtain wheel angular positions. Six 120-Hz Peak Performance optical cameras were used to acquire raw kinematic data. Both kinematic and kinetic data were synchronized and collected for 10 sec. The propulsion phase was defined as the period when the  $M_z$  (moment in z' direction) deviated  $\pm 5\%$  from baseline, until it once again returned to baseline (Cooper et al. 1997). The contact point between the hand and pushrim (point of force application) was determined using kinematic data by assuming it coincides with the MCP2. Three propulsion cycles were normalized and averaged. Mean pushrim forces were obtained from custom software written using MATLAB (The MathWorks Inc., Natick, MA).

## RESULTS

## Static Testing

Linearity and coefficients of determinations ( $r^2$ ) of resultant force ( $F_{x'y'}$ ) and axial force ( $F_{z'}$ ) were presented in Table 1. The IWS demonstrated a high linearity of the force channels ( $0.910 < \text{slope} < 1.410$  and  $r^2 > 0.999$ ). Precision and percent error of IWS compared with each reference force are listed in Table 2. Precision was found to range from 0.24 to 0.54 for  $F_{x'y'}$ , and from 0.14 to 0.54 for  $F_{z'}$ . Percent error of the IWS during static condition was less than 2.72%.

## Dynamic Testing

Linearity and coefficients determinations ( $r^2$ ) of the computed force values from the inverse dynamics method compared with measured forces from IWS are presented in Table 3. High linearity and  $r^2$  also were found during dynamic validation ( $0.969 < \text{slope} < 1.077$  and  $r^2 > 0.811$ ). Precision and percent error for the computed in-plane forces ( $F_X$  and  $F_Y$ , perpendicular to each other) from inverse dynamics method vs. measured forces from the IWS are presented in Table 4. The precision of the IWS was decreased when the weight of the metal block increased. In addition, the highest

**TABLE 1** Linearity and Coefficients of Determinations of  $F_{x'y'}$  and  $F_{z'}$  at Different Reference Positions

Position (axis)	Linearity		$R^2$	
	$F_{x'y'}$	$F_{z'}$	$F_{x'y'}$	$F_{z'}$
x	0.937	1.383	0.999	0.999
xy	0.919	1.309	0.999	0.999
y	0.946	1.297	0.999	0.999
-xy	0.910	1.263	0.999	0.999
-x	0.933	1.358	0.999	0.999
-x-y	0.910	1.399	0.999	0.999
-y	0.942	1.401	0.999	0.999
x-y	0.912	1.410	1.000	0.999

**TABLE 2** Precision and Percent Error at Different Reference Forces

Reference forces (N)	Precision		Error (%)	
	$F_{x'y'}$	$F_{z'}$	$F_{x'y'}$	$F_{z'}$
22.23	0.54	0.54	2.18	2.52
44.45	0.44	0.14	2.71	2.85
66.68	0.44	0.28	2.44	2.39
88.90	0.24	0.39	2.18	1.99
111.13	0.30	0.30	2.12	1.94

**TABLE 3** Linearity and Coefficients of Determination ( $r^2$ ) for the Computed Forces ( $F_X$  and  $F_Y$ ) From Inverse Dynamics Method vs. Measured Forces From Instrumented Wheel System of Two Different Weights Rotated at 1.46 and 7.15 rad/s

Angular velocity (rad·s <sup>-1</sup> )	Weight (Kg)	Linearity		$r^2$	
		$F_X$	$F_Y$	$F_X$	$F_Y$
1.46	2.04	1.003	0.995	0.835	0.895
	3.48	1.077	0.969	0.869	0.811
7.15	2.04	1.000	0.998	0.993	0.986
	3.48	1.000	0.991	0.975	0.992

**TABLE 4** Precision and Percent Error for the Computed Forces ( $F_X$  and  $F_Y$ ) from Inverse Dynamics Method vs. Measured Forces from the IWS of two Different Weights Rotated at 1.46 and 7.15 rad/s

Angular velocity (rad·s <sup>-1</sup> )	Weight (Kg)	Precision		Error (%)	
		$F_X$	$F_Y$	$F_X$	$F_Y$
1.46	2.04	0.29	0.26	0.75	1.43
	3.48	1.24	1.19	1.37	2.66
7.15	2.04	0.55	0.95	2.24	1.43
	3.48	1.93	1.43	4.31	3.61

percent error was found to be 4.31% at the high angular velocity with the heaviest metal block attached to the pushrim.

### 3-D Pushrim Forces

Mean 3-D pushrim forces from the three consecutive strokes are presented in Figure 6. These showed that  $F_r$  reached its peak at 166.17 N, which was higher than the peak  $F_t$  (102.02 N) while the maximum axial force was approximately 48.67 N.

## DISCUSSION

The IWS developed in this study was the first device designed to measure 3-D pushrim forces during racing wheelchair propulsion. The validity and reliability of this racing chair IWS were determined and reported. Although several instrumented wheel force measurement systems have been developed, few studies report the accuracy and properties of their instrumented wheels (Cooper et al. 1997; Goosey-Tolfrey et al. 2001). Cooper et al. (1997) reported a 3% error of the SMART<sup>wheel</sup> during the dynamic condition, while the percent linearity of static forces and moments of the SMART<sup>wheel</sup> were 98.9% and 99.1%, respectively, in conventional wheelchair propulsion.

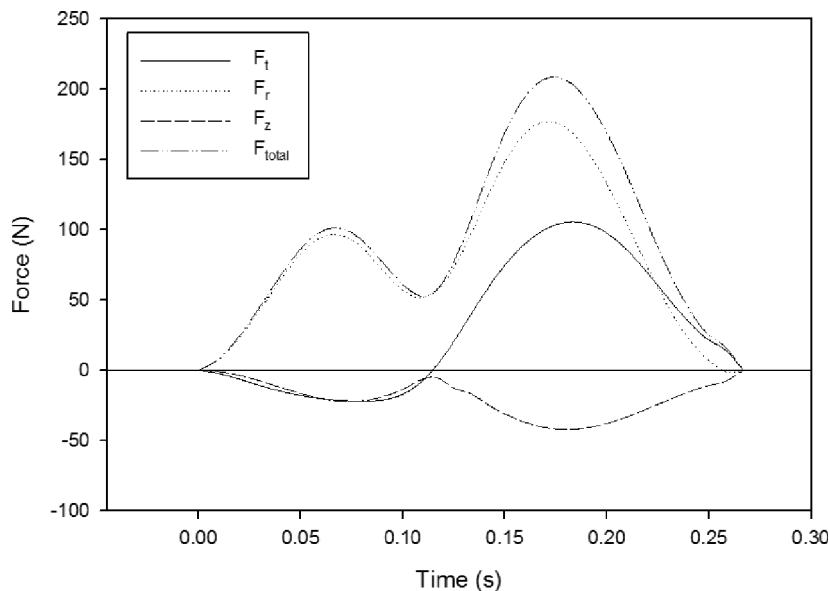


**FIGURE 6** 3-D pushrim forces during three consecutive strokes at the athlete's comfortable speed ( $4.4 \text{ m}\cdot\text{s}^{-1}$ :  $F_t$ : tangential force,  $F_r$ : radial force,  $F_z$ : axial force).

In addition, the precisions were found to be  $0.6 \text{ N}$  for force and  $0.6 \text{ N}\cdot\text{m}$  for moments. The instrumented wheel system developed by Wu et al. (1998) using a 3-D commercial force transducer showed a high linearity ( $0.973 < \text{slope} < 1.015$  and  $r^2 > 0.999$ ). The maximum deviations were found to be  $0.4 \text{ N}$  for force and  $0.08 \text{ N}\cdot\text{m}$  for moment in static condition. However, no precision and percent errors were reported.

Both static and dynamic testing has shown that the IWS developed in this study can be used to measure 3-D pushrim forces with acceptable accuracy. The IWS has been found to have high linearity and is highly correlated to reference forces for both static and dynamic conditions. The highest percent error was found under dynamic conditions (percent error = 4.31%). The high discrepancies for dynamic validation, particularly at the high angular velocity, may be due to the accuracy of the wheel angular position obtained from the kinematic data. The accuracy of the wheel angular position could be improved by incorporating a potentiometer as an angle encoder, which can provide a more accurate wheel angular position during wheel rotation. Moreover, this angle encoder may replace the kinematic system if only 3-D pushrim forces or a percentage of stroke effectiveness need to be obtained.

For the 3-D pushrim forces, the peak  $F_t$  and  $F_z$  found in this study were lower than the peak forces previously reported by Goosey-Tolfrey et al. (2001), who reported the peak of  $F_t$  and  $F_z$  during racing wheelchair propulsion of six experienced wheelchair racers at the speed of  $5.64 \text{ m/s}$  to be

158 N and 82 N, respectively. The difference of these forces between two studies may be due to several factors such as pathology of participants, wheelchair type, racing wheelchair design, and propulsion speed.

Based on the design, this IWS has several advantages. For example, it can be used interchangeably with other standard racing wheelchair frames (1.11 cm axles), and with further validation, this IWS may be adapted to various pushrim sizes. With these features, the IWS would allow wheelchair athletes to be tested in their own racing wheelchairs and their comfortable pushrim sizes, which may provide for a more comfortable and natural propulsion stroke.

In the current study, it is assumed that functional characteristics of the commercial force transducer have been verified from the factory. Thus, we are not interested in validating the force transducer itself, but its application in measuring forces at the pushrim. Only force components of IWS were validated at this time, since we mainly are interested in the joint reaction force prediction. The measurement and calibration of 3D moments may be explored in the future study. The weight of the interface plate can influence the rotating inertia during the wheelchair propulsion. In addition, accurate dynamic validation of the system is a time consuming, very complicated procedure, and it is hard to achieve since the force transducer coordinate system continuously changes its orientation (Wu et al., 1998).

In conclusion, this study presented a first attempt to design a wheel instrument to measure 3-D pushrim forces of wheelchair propulsion in a racing wheelchair. With available commercial 3-D force and moment transducers, this instrument would provide ideas for different research groups when constructing an IWS to measure pushrim forces in various settings. In addition, the IWS can further be improved by installing a wireless communication system or a data logger in order to collect data during training or competition in the field.

## REFERENCES

- Asato KT, Cooper RA, Robertson RN, Ster JF (1993) Smartwheels: Development and testing of a system for measuring manual wheelchair propulsion dynamics. *IEEE Trans Biomed Eng* 40(12): 1320–1324.
- Cooper RA (1995) *Rehabilitation engineering: Applied to mobility and manipulation*. Philadelphia: IOP Publishing Ltd.
- Cooper RA, Robertson RN, VanSickle DP, Boninger ML, Shimada SD (1997) Methods for determining three-dimensional wheelchair pushrim forces and moments: A technical note. *J Rehabil Res Dev* 34(2): 162–170.
- Finley MA, Rasch EK, Keyser RE, Rodgers MM (2004) The biomechanics of wheelchair propulsion in individuals with and without upper-limb impairment. *J Rehabil Res Dev* 41(3B): 385–395.

- Goosey-Tolfrey VL, Fowler NE, Campbell IG, Iwnicki SD (2001) A kinetic analysis of trained wheelchair racers during two speeds of propulsion. *Med Eng Phys* 23(4): 259–266.
- VanSickle DP, Cooper RA, Robertson RN (1995). *Smartwheel: Development of a digital force and moment sensing pushrim*. Paper presented at the Annual Conference of Rehabilitation Engineering & Assistive Technology Society of North America.
- Wu HW, Berglund LJ, Su FC, Yu B, Westreich A, Kim KJ, An KN (1998) An instrumented wheel for kinetic analysis of wheelchair propulsion. *J Biomech Eng* 120(4): 533–535.